Fundamental Physics and Gravitational Waves

Riccardo Sturani

International Institute of Physics - UFRN - Natal (Brazil)

USP, June 3rd 2020

GW basics in 1 slide

Gauged fixed metric perturbations $h_{\mu\nu}$ after discarding $h_{0\mu}$ components, which are not radiative $\rightarrow$ transverse waves

$$h_{ij} = \begin{pmatrix} h_+ & h_\times & 0 \\ h_\times & -h_+ & 0 \\ 0 & 0 & 0 \end{pmatrix}$$

2 pol. state like any mass-less particle

h_+

$h_\times$

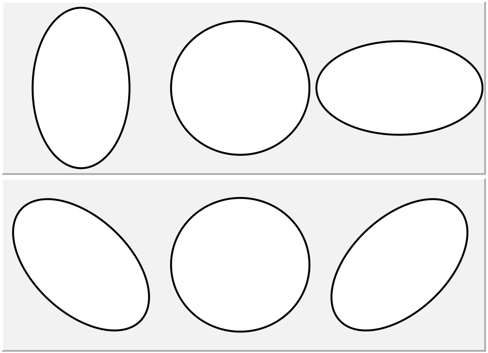

LIGO and Virgo: very precise rulers

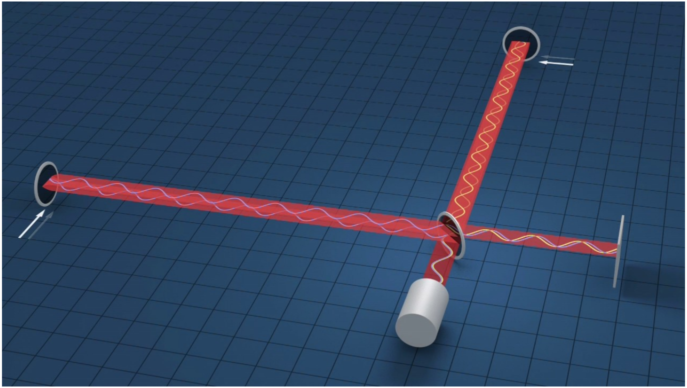

Robert Hurt (Caltech)

Light intensity $\propto$ light travel difference in perpendicular arms
Effective optical path increased by factor $N \sim 500$ via Fabry-Perot cavities

Phase shift $\Delta\phi \sim 10^{-8}$ can be measured $\sim 2\pi N \Delta L/\lambda \rightarrow \Delta L \sim 10^{-15}/N$ m

Almost omnidirectional detectors

Detectors measure h_{det}: linear combination $F_+ h_+ + F_\times h_\times$

L $\qquad\qquad\qquad\qquad$ H

-1 0 1

F_+

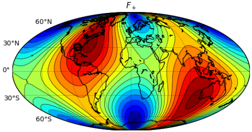

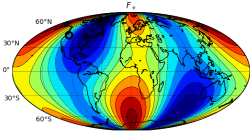

$F_\times$

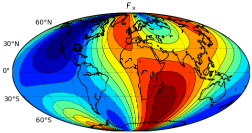

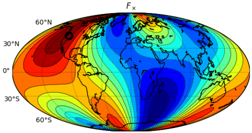

$h_{+,\times}$ depend on source

pattern functions $F_{+,\times}$ depend on orientation source/detector

Almost omnidirectional detectors

Detectors measure h_{det}: linear combination $F_+ h_+ + F_\times h_\times$

L V

-1 0 1

F_+

$F_\times$

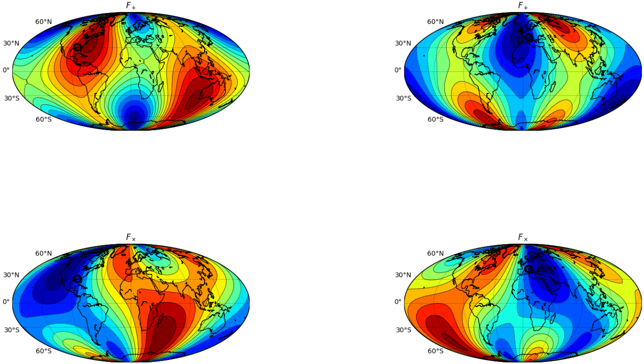

$h_{+,\times}$ depend on source

pattern functions $F_{+,\times}$ depend on orientation source/detector

Pattern functions: $\sqrt{F_+^2 + F_\times^2}$

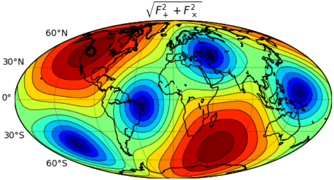

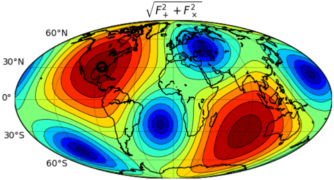

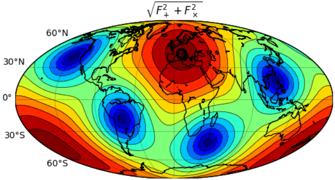

The LIGO and Virgo observatories

- Observation run **O1** Sept '15 - Jan '16
$\sim$ 130 days, with 49.6 days of actual data, PRX (2016) 4, 041014, 2 detectors, 3BBH
- **O2** Dec. '16 – Jul'17 2 det's + Aug '17 3 det's
3(+4) BBH + 1BNS in double (triple) coinc.
- **O3a**: 3 detectors, Apr 2nd - Oct 1st 2019
- **O3b**: Nov 1st – Mar/2020

In April 2020 Japanese KAGRA joined the network, in 202? Indian INDIGO will join the collab-

Wave generation: localized sources

Einstein formula relates h_{ij} to the source quadrupole moment Q_{ij}

$$\begin{aligned} Q_{ij} &= \int d^3x\rho\left(x_ix_j - \frac{1}{3}\delta_{ij}x^2\right)\,, \qquad v^2 \simeq G_N M/r\,, \quad \eta \equiv m_1 m_2/M^2 \\ h_{ij} &\sim g(\theta_{LN})\frac{2G_N}{D}\frac{d^2Q_{ij}}{dt^2} \simeq \frac{2G_N\eta M v^2}{D}\cos(2\phi(t)) \end{aligned}$$

$$\begin{aligned} f &= 2\mathrm{kHz}\left(\frac{r}{30\mathrm{Km}}\right)^{-3/2}\left(\frac{M}{3M_\odot}\right)^{1/2} < f_{Max} \simeq 12kHz\left(\frac{M}{3M_\odot}\right)^{-1} \\ v &= 0.3\left(\frac{f}{1\mathrm{kHz}}\right)^{1/3}\left(\frac{M}{M_\odot}\right)^{1/3} < \frac{1}{\sqrt{6}} \end{aligned}$$

Geometric factor $g(\theta_{LN})$ takes account of transversality projection (angular momentum L of the binary, observation direction N)

$$\begin{aligned} h_+ &\sim \frac{1+\cos^2(\theta_{LN})}{2}\eta\frac{Mv^2}{D}\cos\phi(t_s/M,\eta,S_i^2/m_i^4,\ldots) \\ h_\times &\sim \cos(\theta_{LN})\,\eta\frac{Mv^2}{D}\sin\phi(t_s/M,\eta,\ldots) \end{aligned}$$

Amplitudes of 2 polarizations modulated by θ_{LN} ($h \nearrow$ for $\theta_{LN} \searrow_0$), never both vanishing unlike dipolar motion for the electromagnetic case

Wave generation: localized sources

Einstein formula relates h_{ij} to the source quadrupole moment Q_{ij}

$$
\begin{aligned}
Q_{ij} &= \int d^3x\rho\left(x_ix_j-\frac{1}{3}\delta_{ij}x^2\right)\,, \qquad v^2\simeq G_N M/r\,,\quad \eta\equiv m_1m_2/M^2\\
h_{ij} &\sim g(\theta_{LN})\frac{2G_N}{D}\frac{d^2Q_{ij}}{dt^2}\simeq\frac{2G_N\eta M v^2}{D}\cos(2\phi(t))
\end{aligned}
$$

$$
\begin{aligned}
f &= 2\mathrm{kHz}\left(\frac{r}{30\mathrm{Km}}\right)^{-3/2}\left(\frac{M}{3M_\odot}\right)^{1/2} < f_{Max}\simeq 12kHz\left(\frac{M}{3M_\odot}\right)^{-1}\\
v &= 0.3\left(\frac{f}{1\mathrm{kHz}}\right)^{1/3}\left(\frac{M}{M_\odot}\right)^{1/3} < \frac{1}{\sqrt{6}}
\end{aligned}
$$

Geometric factor $g(\theta_{LN})$ takes account of transversality projection (angular momentum L of the binary, observation direction N)

$$
\begin{aligned}
h_+ &\sim \frac{1+\cos^2(\theta_{LN})}{2}\,\eta\frac{M(1+z)v^2}{D(1+z)}\cos\phi(t_O/(M(1+z)),\eta,S_i^2/m_i^4,\ldots)\\
h_\times &\sim \cos(\theta_{LN})\,\eta\frac{M(1+z)v^2}{D(1+z)}\sin\phi(t_O/(M(1+z)),\eta,\ldots)
\end{aligned}
$$

Amplitudes of 2 polarizations modulated by θ_{LN} ($h\nearrow$ for $\theta_{LN}\searrow_0$), never both vanishing unlike dipolar motion for the electromagnetic case

Wave generation: localized sources

Einstein formula relates h_{ij} to the source quadrupole moment Q_{ij}

$$
\begin{aligned}
Q_{ij} &= \int d^3x\rho\left(x_ix_j - \frac{1}{3}\delta_{ij}x^2\right)\,, \qquad v^2 \simeq G_N M/r\,, \quad \eta \equiv m_1 m_2/M^2 \\
h_{ij} &\sim g(\theta_{LN})\frac{2G_N}{D}\frac{d^2Q_{ij}}{dt^2} \simeq \frac{2G_N\eta M v^2}{D}\cos(2\phi(t)) \\
f &= 2\mathrm{kHz}\left(\frac{r}{30\mathrm{Km}}\right)^{-3/2}\left(\frac{M}{3M_\odot}\right)^{1/2} < f_{Max} \simeq 12kHz\left(\frac{M}{3M_\odot}\right)^{-1} \\
v &= 0.3\left(\frac{f}{1\mathrm{kHz}}\right)^{1/3}\left(\frac{M}{M_\odot}\right)^{1/3} < \frac{1}{\sqrt{6}}
\end{aligned}
$$

Geometric factor $g(\theta_{LN})$ takes account of transversality projection (angular momentum L of the binary, observation direction N)

$$
\begin{aligned}
h_+ &\sim \frac{1+\cos^2(\theta_{LN})}{2}\,\eta\frac{\mathcal{M}v^2}{d_L}\cos\phi(t_O/\mathcal{M},\eta,S_i^2/m_i^4,\ldots) \\
h_\times &\sim \cos(\theta_{LN})\,\eta\frac{\mathcal{M}v^2}{d_L}\sin\phi(t_O/\mathcal{M},\eta,\ldots)
\end{aligned}
$$

Amplitudes of 2 polarizations modulated by θ_{LN} ($h \nearrow$ for $\theta_{LN} \searrow_0$), never both vanishing unlike dipolar motion for the electromagnetic case

h sensitive to red-shifted masses $M \to M(1+z) \equiv \mathcal{M}$

Binary systems and compact detected so far

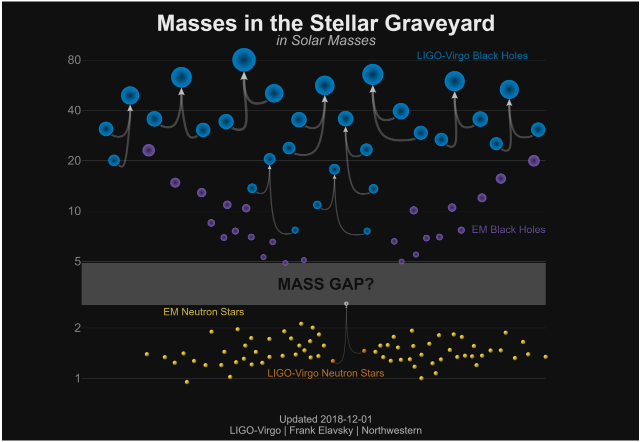

1. GW190412: sistema mais asimetrico: $m_1/m_2 \sim 3$, massa total $\sim 40 M_\odot$
2. GW190425: novo sistema binário de estrela de nêutrons

Sky localization

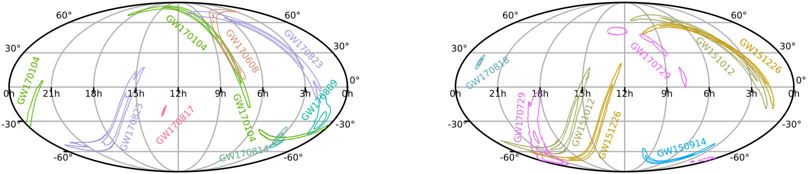

Distances between 40 e $\sim 2800\,Mpc$ ($\pm 20\%$), (our galaxy size $\sim 30\mathrm{kpc}$)

Image by Leo Singer, http://www.ligo.org

GW170817

- GW trigger on Aug 17th, 2017, ended at 12h 41' 04.4" UTC, first in in LIGO Hanford, then confirmed as a triple coincidence $\rightarrow$ localized in an area of $\sim$ 28 deg^2
- GRB trigger from Fermi-GBM 1.7" after
- first optical image 10.87 hr afterwards by One-Meter Two Hemisphere team with Swope telescope at Las Campanas Observatory in Chile
- X obtained by the X-Ray Telescope on Swift after 14.9 h (NuSTAR 16.8 h)
- radio ($\sim 3,6$ GHz) by VLA 16 days after GW event

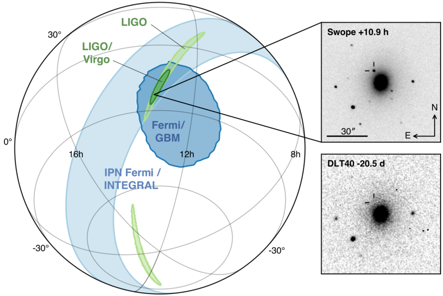

LIGO/Virgo & Partner Astronomy groups, Astrophys.J. 848 (2017) no.2, L12

An example of the optical image

Transient Optical Robotic Observatory of the South 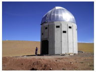

GW170817 and ν detectors

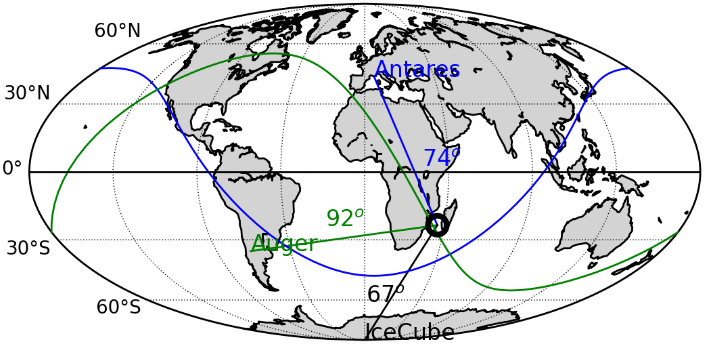

Potential νs down-going for Antares and IceCube, grazing for Auger

GW170817 and ν detectors

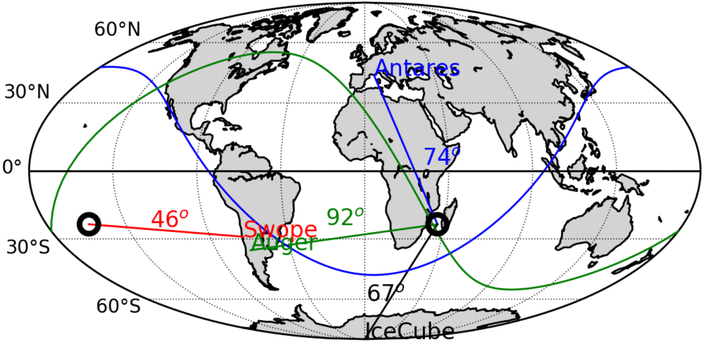

Potential νs down-going for Antares and IceCube, grazing for Auger

Source location at optical detection

ANTARES and ICECube look for ν

IceCube and ANTARES looked for $\mu - \nu$ at $\pm 500 sec$, observation for 2 weeks

no detection

Pierre Auger for $> 10^{17}$ eV, grazing good for τ production at 10^{18} eV

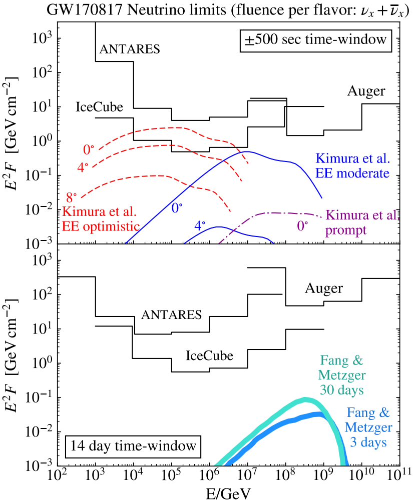

LIGO/Virgo, ANTARES, ICECUBE and Pierre Auger, Astrophys.J. 850 '17 2, L35

Event	Primary mass (M_sun)	Secondary mass (M_sun)	Effective inspiral spin	chirp mass (M_sun)	Final spin	Final mass (M_sun)	Luminosity distance (Mpc)	Sky localization (deg^2)
GW150914	$35.6^{+4.8}_{-3.0}$	$30.6^{+3.0}_{-4.4}$	$-0.01^{+0.12}_{-0.13}$	$28.6^{+1.6}_{-1.5}$	$0.69^{+0.05}_{-0.04}$	$63.1^{+3.3}_{-3.0}$	430^{+150}_{-170}	179
GW151012	$23.3^{+14.0}_{-5.5}$	$13.6^{+4.1}_{-4.8}$	$0.04^{+0.28}_{-0.19}$	$15.2^{+2.0}_{-1.1}$	$0.67^{+0.13}_{-0.11}$	$35.7^{+9.9}_{-3.8}$	1060^{+540}_{-480}	1555
GW151226	$13.7^{+8.8}_{-3.2}$	$7.7^{+2.2}_{-2.6}$	$0.18^{+0.20}_{-0.12}$	$8.9^{+0.3}_{-0.3}$	$0.74^{+0.07}_{-0.05}$	$20.5^{+6.4}_{-1.5}$	440^{+180}_{-190}	1033
GW170104	$31.0^{+7.2}_{-5.6}$	$20.1^{+4.9}_{-4.5}$	$-0.04^{+0.17}_{-0.20}$	$21.5^{+2.1}_{-1.7}$	$0.66^{+0.08}_{-0.10}$	$49.1^{+5.2}_{-3.9}$	960^{+430}_{-410}	924
GW170608	$10.9^{+5.3}_{-1.7}$	$7.6^{+1.3}_{-2.1}$	$0.03^{+0.19}_{-0.07}$	$7.9^{+0.2}_{-0.2}$	$0.69^{+0.04}_{-0.04}$	$17.8^{+3.2}_{-0.7}$	320^{+120}_{-110}	396
GW170729	$50.6^{+16.6}_{-10.2}$	$34.3^{+9.1}_{-10.1}$	$0.36^{+0.21}_{-0.25}$	$35.7^{+6.5}_{-4.7}$	$0.81^{+0.07}_{-0.13}$	$80.3^{+14.6}_{-10.2}$	2750^{+1350}_{-1320}	1033
GW170809	$35.2^{+8.3}_{-6.0}$	$23.8^{+5.2}_{-5.1}$	$0.07^{+0.16}_{-0.16}$	$25.0^{+2.1}_{-1.6}$	$0.70^{+0.08}_{-0.09}$	$56.4^{+5.2}_{-3.7}$	990^{+320}_{-380}	340
GW170814	$30.7^{+5.7}_{-3.0}$	$25.3^{+2.9}_{-4.1}$	$0.07^{+0.12}_{-0.11}$	$24.2^{+1.4}_{-1.1}$	$0.72^{+0.07}_{-0.05}$	$53.4^{+3.2}_{-2.4}$	580^{+160}_{-210}	87
GW170817	$1.46^{+0.12}_{-0.10}$	$1.27^{+0.09}_{-0.09}$	$0.00^{+0.02}_{-0.01}$	$1.186^{+0.001}_{-0.001}$	≤ 0.89	≤ 2.8	40^{+10}_{-10}	16
GW170818	$35.5^{+7.5}_{-4.7}$	$26.8^{+4.3}_{-5.2}$	$-0.09^{+0.18}_{-0.21}$	$26.7^{+2.1}_{-1.7}$	$0.67^{+0.07}_{-0.08}$	$59.8^{+4.8}_{-3.8}$	1020^{+430}_{-360}	39
GW170823	$39.6^{+10.0}_{-6.6}$	$29.4^{+6.3}_{-7.1}$	$0.08^{+0.20}_{-0.22}$	$29.3^{+4.2}_{-3.2}$	$0.71^{+0.08}_{-0.10}$	$65.6^{+9.4}_{-6.6}$	1850^{+840}_{-840}	1651

https://www.gw-openscience.org/catalog/

See however Princeton's group results arXiv:1904.07214

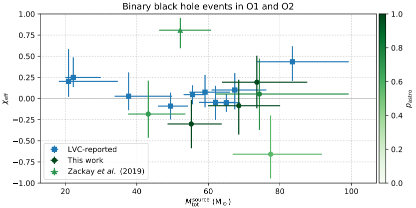

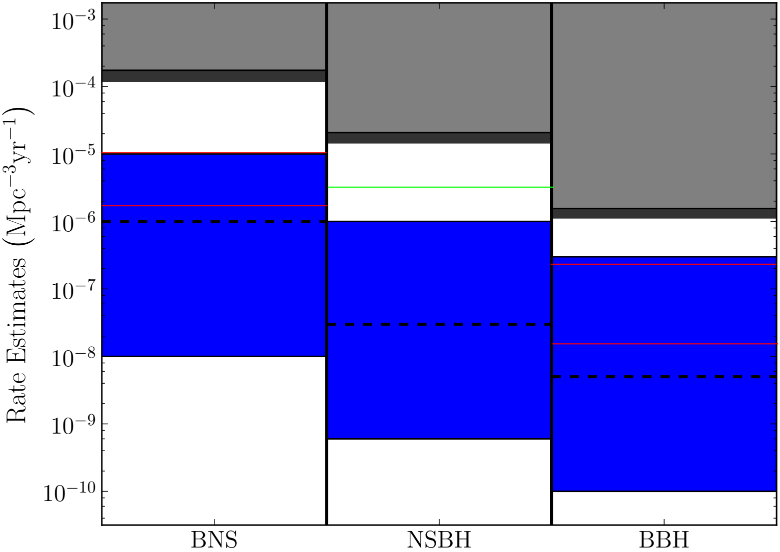

Astrophysical predictions, upper limit from S5/6/O1 and observation from O1/O2

LIGO/Virgo CQG ('10) 27 173001, PRX ('16), APJ (2016), PRL 119 ('17)

Ongoing O3: towards measuring merger distribution

At https://gracedb.ligo.org/superevents/public/O3
summary of candidate detections from O3a+b:
1 BNS+1BBH+53(+1) candidate events, $\sim$ 10 of which possibly involving at least a NS

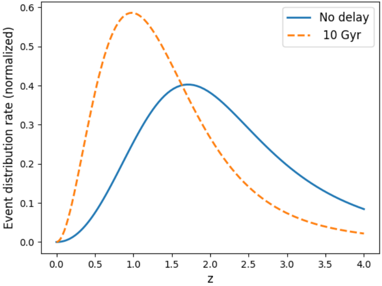

Expected merger distribution from Star Formation Rate (—) or SFR+Poissian distributed delay (– –)

Ongoing O3: towards measuring merger distribution

At https://gracedb.ligo.org/superevents/public/O3
summary of candidate detections from O3a+b:
1 BNS+1BBH+53(+1) candidate events, $\sim$ 10 of which possibly involving at least a NS

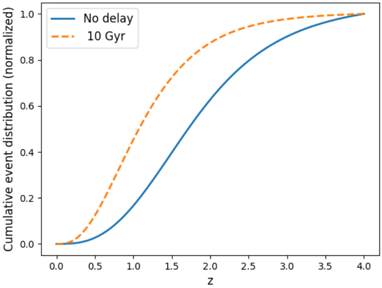

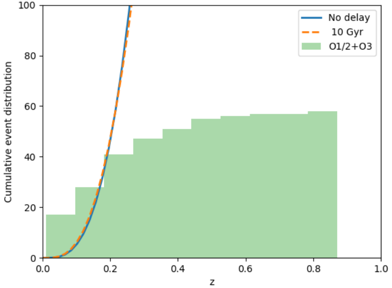

Expected merger distribution from Star Formation Rate (—) or SFR+Poissian distributed delay (– –)

Future with ET and LISA looks very loud

Future 3rd generetaion detectors (Einstein Telescope, Cosmic Explore)/space telescope LISA will detect CBC signals with SNR $10 - 10^2$, with few golden events with SNR $\sim 10^3$.

Templates few % accurate OK for characterising a source with SNR $O(10)$ (typical for LIGO/Virgo)

for SNR $\sim 10^3$ residual after extracting that source will have SNR $\sim O(10)$

1. baising parameter estimation
2. contaminating the extraction of additional sources.

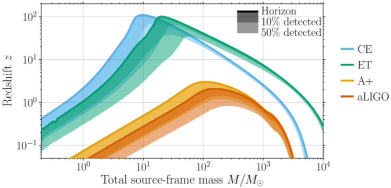

from arXiv:1902.09485

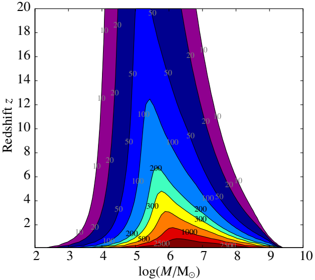

from arXiv:1201.3621

How many more?

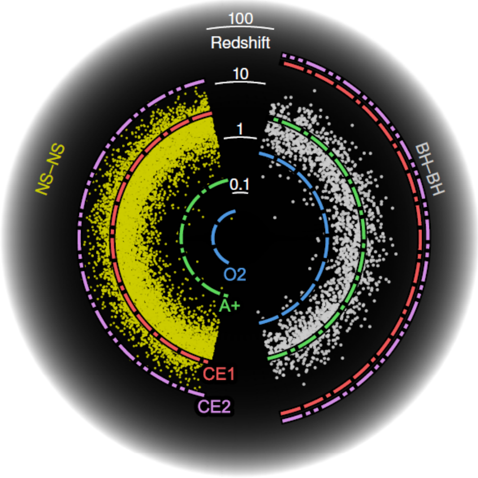

arXiv:1903.04615

New lines of research

- Precision gravity
- General Relativity tests in strong gravity
- "Hairiness" of black holes
- Universe expansion history (standard sirens)
- Phase transitions in the Early Universe
- Black hole mass function
- How binary systems form and how frequent are they? (star formation rate)
- Fate of a massive star
- Probe the the interior of a neutron star
- Understand the life of a pulsar and its evolution
- Dark matter and Gravitational Waves (modification of compact object and/or their environment)
- Data analysis challenges for signals with $SNR \sim 100$
- Central Core of Galaxies, Massive Black Holes and their role in Galaxy Formation
- Multi-messenger astronomy

New lines of research

- Precision gravity
- General Relativity tests in strong gravity
- "Hairiness" of black holes
- Universe expansion history (standard sirens)
- Phase transitions in the Early Universe
- Black hole mass function
- How binary systems form and how frequent are they? (star formation rate)
- Fate of a massive star
- Probe the the interior of a neutron star
- Understand the life of a pulsar and its evolution
- Dark matter and Gravitational Waves (modification of compact object and/or their environment)
- Data analysis challenges for signals with $SNR \sim 100$
- Central Core of Galaxies, Massive Black Holes and their role in Galaxy Formation
- Multi-messenger astronomy

The importance of theoretical modeling

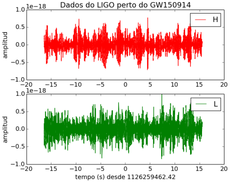

×

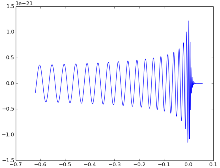

/

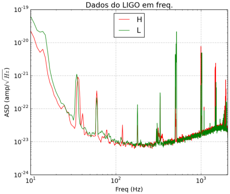

2

The importance of theoretical modeling

2

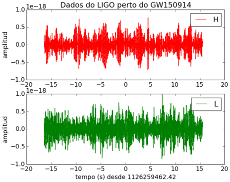

×

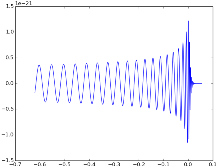

/

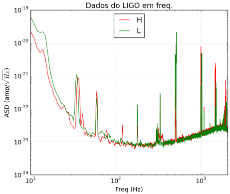

=

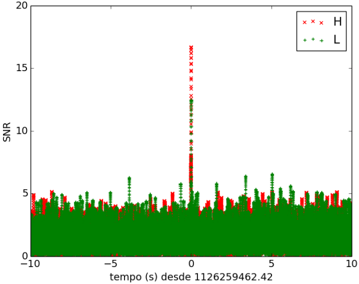

Data from https://losc.ligo.org/events/GW150914/

Fundamental GR: inspiral analytic model

Inspiral $h = A\cos(\phi(t))$ $\qquad \frac{\dot{A}}{A} \ll \dot{\phi}$

Virial relation:

$$v \equiv (G_N M \pi f_{GW})^{1/3} \qquad \eta = \frac{m_1 m_2}{(m_1+m_2)^2}$$

$$\begin{aligned} E(v) &= -\frac{1}{2}\eta M v^2 \left(1 + \#(\eta, S_i/m_i^2)v^2 + \#(\eta, S_i/m_i^2)v^4 + \ldots\right) \\ P(v) \equiv -\frac{dE}{dt} &= \frac{32}{5G_N} v^{10} \left(1 + \#(\eta, S_i/m_i^2)v^2 + \#(\eta, S_i/m_i^2)v^3 + \ldots\right) \end{aligned}$$

E(v)(P(v)) known up to 3(3.5)PN

$$\begin{aligned} \frac{1}{2\pi}\phi(T) &= \frac{1}{2\pi}\int^T \omega(t)dt = -\int^{v(T)} \frac{\omega(v)dE/dv}{P(v)} dv \\ &\sim \int \left(1 + \#(\eta, S_i/m_i^2)v^2 + \ldots + \#(\eta, S_i/m_i^2)v^6 + \ldots\right) \frac{dv}{v^6} \end{aligned}$$

Fundamental GR: inspiral analytic model

Inspiral $h = A\cos(\phi(t))$ $\qquad \frac{\dot{A}}{A} \ll \dot{\phi}$

Virial relation:

$$v \equiv (G_N M \pi f_{GW})^{1/3} \qquad \eta = \frac{m_1 m_2}{(m_1+m_2)^2}$$

$$\begin{aligned} E(v) &= -\frac{1}{2}\eta M v^2 \left(1 + \#(\eta, S_i/m_i^2)v^2 + \#(\eta, S_i/m_i^2)v^4 + \ldots\right) \\ P(v) \equiv -\frac{dE}{dt} &= \frac{32}{5G_N} v^{10} \left(1 + \#(\eta, S_i/m_i^2)v^2 + \#(\eta, S_i/m_i^2)v^3 + \ldots\right) \end{aligned}$$

E(v)(P(v)) known up to 3(3.5)PN

$$\begin{aligned} \frac{1}{2\pi}\phi(T) &= \frac{1}{2\pi}\int^T \omega(t)dt = -\int^{v(T)} \frac{\omega(v)dE/dv}{P(v)} dv \\ &\sim \int \left(1 + \#(\eta, S_i/m_i^2)v^2 + \ldots + \#(\eta, S_i/m_i^2)v^6 + \ldots\right) \frac{dv}{v^6} \end{aligned}$$

PN Coefficients (tidal $\sim v^{10}$)

PN approximation to General Relativity

Small expansion parameter v, related to metric perturbation $v^2 \sim \frac{G_N M}{r}$

Near zone, $D \sim r$

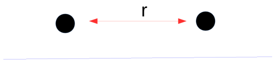

Describe conservative dynamics

Far zone, $D \gtrsim \lambda = r/v$

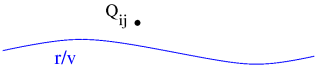

conservative + dissipative

EFT framework pioneered by W. Goldberger and I. Rothstein, PRD '06

Newtonian potential:

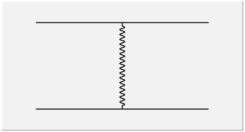

$$S_{eff} \sim \int dt \, \frac{G_N m_1 m_2}{r} \sim L$$

At 1PN:

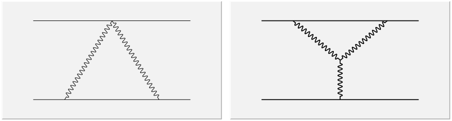

$$S_{eff} = \int dt \, \frac{G_N^2 m_1^2 m_2}{r^2} \sim L v^2$$

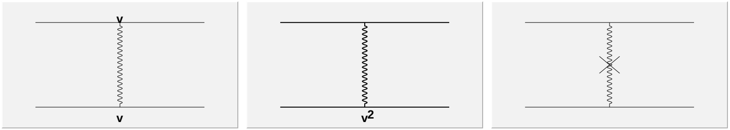

$$V_{1PN} = -\frac{G m_1 m_2}{2r}\left[1 - \frac{G_N m_1}{2r} + \frac{3}{2}(v_1^2) - \frac{7}{2} v_1 v_2 - \frac{1}{2} v_1 \hat{r} v_2 \hat{r}\right] + 1 \leftrightarrow 2$$

Different approximation methods

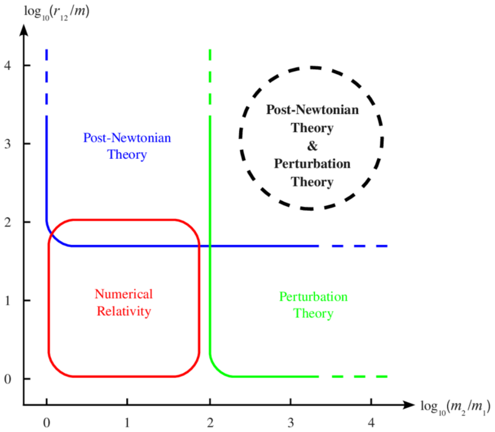

(Blanchet et al. arXiv:1007.2614)

Numerical relativity solution are expensive for large separation (large orbital scale) and large mass ratios (long dynamical evolution time)

Looking for sources fingerprints

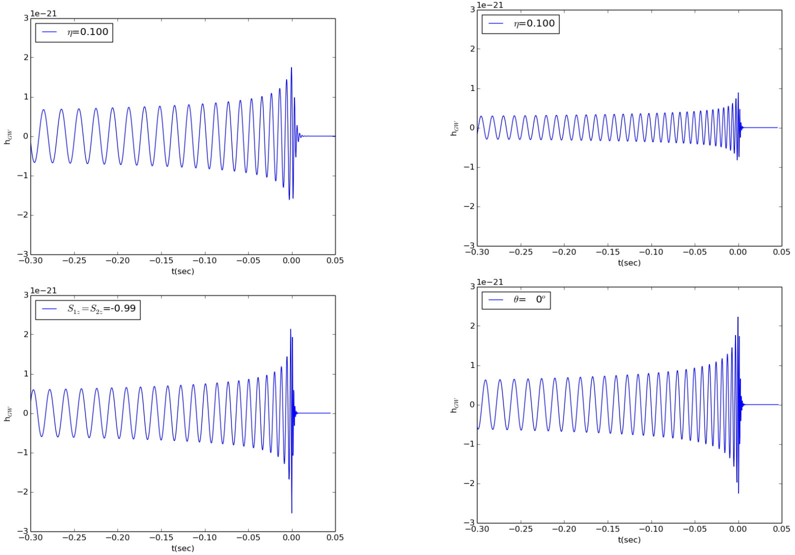

Testing the PN series with O1/2

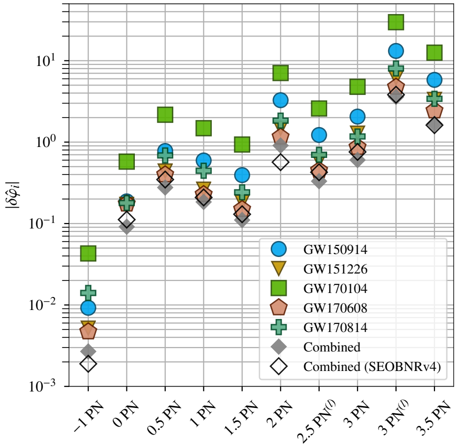

Precision in measuring the PN coefficients $\sim 100\%$: one cannot both measure the astro parameters and test GR with same detection! Unique probe of high PN-orders

LIGO/Virgo arXiv:1903.04467

Tidal deformability $\Lambda \simeq R^{-5} Q_{ab} / (\partial_a \partial_b U_{tidal})$ depends on Equation of State

Determinaton of $\Lambda_{1,2}$
(assuming same EoS for 1,2)

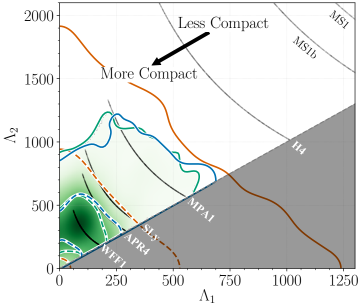

Shading Common EoS for 2 bodies and constrain for $m_{max} > 1.97 M_\odot$
Lines 50%, 90% countours, No mimimum m_{max}, independent EoSs

LIGO/Virgo collaboration, arXiv:1805.11581

Fundamental physics of Neutron stars II

Parametrizing EoS with $\Gamma \equiv \frac{\epsilon+p}{p}\frac{dp}{d\epsilon}$, $\Gamma(x) = \exp\left(\sum_k \gamma_k x^k\right)$, $\quad x \equiv \log \frac{p}{p_0}$

$$\gamma_0 \in [0.2, 2], \gamma_1 \in [1.6, 1.7], \gamma_2 \in [0.6, 0.6] \gamma_3 \in [0.02, 0.02], \Gamma(p) \in [0.6, 4.5]$$

L. Lindblom PRD 82, 103011 (2010)

Constraints on Mass vs- radius and p vs. rho

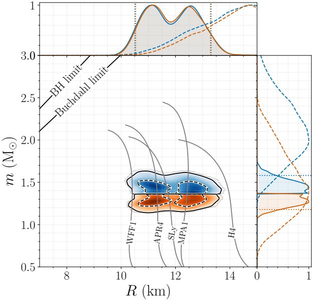

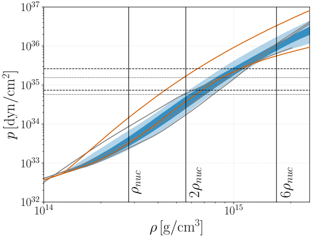

lighter, heavier

90% prior, posterior

LIGO/Virgo collaboration, arXiv:1805.11581

Cosmology

- From GWs only: luminosity distance $d_L \sim 40^{+8}_{-14}$Mpc, viewing angle $\theta_{LN} > 125^o$
- Fixing d_L from info from EM location + Hubble relation $d_L H_0 = z$
  1. Hubble constant from SuperNovae (SHoES) $148^o < \theta_{LN} < 166^o$

     Riess et al. ApJ 826, 56 '16
  2. from Planck $157 < \theta_{LN} < 177^o$

     Planck A&A, 594, A13 '16
- GW almost coincident with EM $\implies \Delta v_{GW}/c \sim 10^{-15}$ LIGO/Virgo, Fermi Gamma-Ray Burst Monitor, INTEGRAL Ap.J. 848 (2017) 2, L13

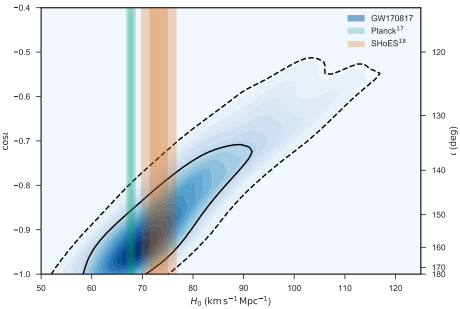

LIGO/Virgo Nature 551 '17 7678, 85

$$h''_{+\times} + 2\frac{a'}{a} h'_{+,\times} + c_s^2 \nabla^2 h_{+,\times} = 0$$

Determining H_0 without EM counterpart

Hubble law: $z = H_0 d_L$

D_L can be measured, z degenerate with M, however if

- the source in the sky has been localised (α, δ)
- GW sources are in the galaxy catalogue with known red-shift

$$P(z, D_L|c_i) = \int d\mathcal{M}\, d\vec{\theta}\, d\alpha\, d\delta\, P(D_L \mathcal{M}, \vec{\theta}, \alpha, \delta | c_i)\pi(z, |\alpha, \delta)$$

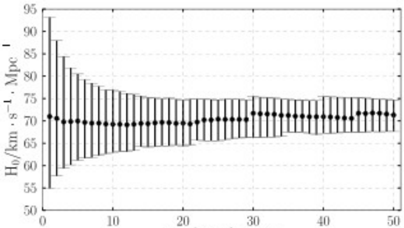

Schutz, Nature (1986) 323 310
W. Del Pozzo, Phys.Rev.D86 (2012) 043011

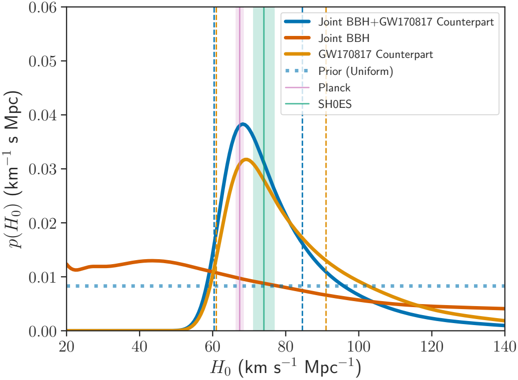

sky localization from DES-Y1 (GW170814)
GWENS (GW170818)
GLADE (GW150914, GW151226, GW170608)

LIGO/Virgo, arXiv:1908.06060

Conclusions (Actually just the beginning!)

- After the beginning of GW astronomy, we have witnessed the start of multi-messenger astronomy
- New era for Cosmology: H_0 from GWs! (and EM)
- New input for fundamental physics: test of gravity in the strong field at short scale, radiative gravity sector tested at large distances and soon precision gravity is going to be needed